Journal Pre-proof

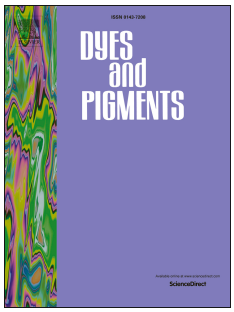

Characterization of the reactivity of luciferin boronate - a probe for inflammatory oxidants with improved stability

Marcin Szala, Aleksandra Grzelakowska, Julia Modrzejewska, Przemysław Siarkiewicz, Daniel Słowiński, Małgorzata Świerczyńska, Jacek Zielonka, Radosław Podsiadły

PII: S0143-7208(20)31390-5

DOI: https://doi.org/10.1016/j.dyepig.2020.108693

Reference: DYPI 108693

To appear in: *Dyes and Pigments*

Received Date: 27 May 2020

Revised Date: 1 July 2020

Accepted Date: 3 July 2020

Please cite this article as: Szala M, Grzelakowska A, Modrzejewska J, Siarkiewicz P, Słowiński D, Świerczyńska M, Zielonka J, Podsiadły R, Characterization of the reactivity of luciferin boronate - a probe for inflammatory oxidants with improved stability, *Dyes and Pigments*, https://doi.org/10.1016/j.dyepig.2020.108693.

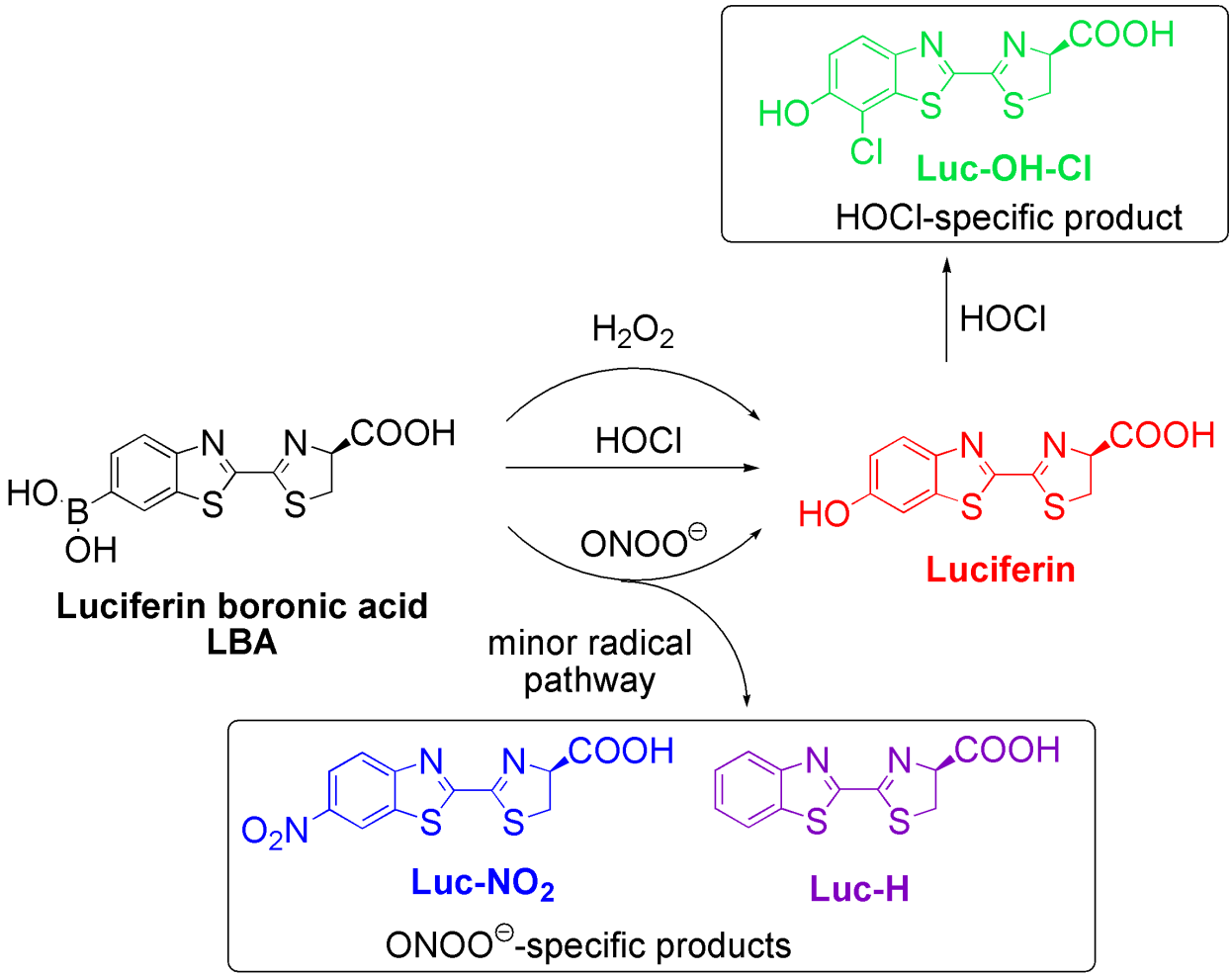
Luc-OH-Cl
HOCl-specific product
HOCl
H_2O_2
HOCl
$ONOO^{\ominus}$
minor radical pathway
Luciferin boronic acid
LBA
Luciferin
Luc-NO_2
Luc-H
$ONOO^{\ominus}$-specific products

Characterization of the reactivity of luciferin boronate - a probe for inflammatory oxidants with improved stability

Marcin Szala[1*], Aleksandra Grzelakowska[1], Julia Modrzejewska[1], Przemysław Siarkiewicz[1], Daniel Słowiński[1], Małgorzata Świerczyńska[1], Jacek Zielonka[2*] and Radosław Podsiadły[1†]

[1] Institute of Polymer and Dye Technology, Faculty of Chemistry, Lodz University of Technology, Stefanowskiego 12/16, 90-924 Lodz, Poland

[2] Department of Biophysics, Medical College of Wisconsin, 8701 Watertown Plank Road, Milwaukee, WI 53226, United States

Abstract

Boronate derivatives of luciferin, containing oxidant-activated self-immolative moieties, recently have been developed for bioluminescent detection of hydrogen peroxide in animal models. Here, we report the synthesis and characterization of luciferin boronic acid pinacol ester (LBE) as a probe for detection of hydrogen peroxide, hypochlorous acid, and peroxynitrite, with improved stability and response time. HPLC analyses showed that LBE quickly hydrolyzes in phosphate buffer to luciferin boronic acid (LBA). Hydrogen peroxide oxidizes LBA slowly, with the formation of luciferase substrate, luciferin (Luc-OH), as the only product. Hypochlorite also oxidizes LBA to luciferin, but the subsequent reaction of Luc-OH with hypochlorite gives a chlorinated luciferin Luc-OH-Cl, which has a higher fluorescence quantum yield than luciferin at pH 7.4 and is also a substrate for luciferase (Takakura H, et. all. ChemBioChem 2012;13:1424). Similar to other boronate probes, LBA is oxidized by peroxynitrite in two pathways. Luc-OH is the product of the major pathway, common for all the oxidants tested, whereas the non-fluorescent nitrated derivative, Luc-NO_2, is formed in the minor pathway, specific for peroxynitrite. Formation of luciferin radical intermediate in the minor pathway has been confirmed by EPR spin trapping and mass spectrometric analyses of the spin adducts. We conclude that LBE shows potential as an improved probe for the detection of inflammatory oxidants in biological settings. Complementation of the bioluminescence measurements by HPLC or LC-MS-based identification of chlorinated and nitrated luciferin(s) will help identify the oxidants detected.

Keywords: luminogenic probes, firefly luciferin-based probe, peroxynitrite-specific product

† Corresponding authors.
E-mail addresses: marcin.szala@p.lodz.pl, jzielonk@mcw.edu, radoslaw.podsiadly@p.lodz.pl, aleksandra.grzelakowska@p.lodz.pl, , julia.modrzejewska@edu.p.lodz.pl, przemyslaw.siarkiewicz@edu.p.lodz.pl, daniel.slowinski@edu.p.lodz.pl, malgorzata.swierczynska@edu.p.lodz.pl

Abbreviations: BLI, bioluminescent imaging; CAT, catalase; CBA, coumarin-7-boronic acid; dppf, 1,1'-ferrocenediyl-bis(diphenylphosphine); DMSO, dimethyl sulfoxide; DPBS, Dulbecco's phosphate-buffered saline; dtpa, diethylenetriaminepentaacetic acid; DMEM, Dulbecco's Modified Eagle Medium; EPR, electron paramagnetic resonance; ESI, electrospray ionization; HO-Bz-OH, 4-hydroxybenzyl alcohol; HPLC, high performance liquid chromatography; Hz, hertz; IFN-γ, interferon γ; iNOS, inducible nitric oxide synthase; isoAmONO, isoamyl nitrite; L-NAME, L-N^G-nitroarginine methyl ester; LBA, luciferin 6'-boronic acid; LBE, luciferin 6'-boronic acid pinacol ester; LC-MS, liquid chromatography-mass spectrometry; LPS, lipopolysaccharide; Luc-Bz$^{\bullet}$, PCL-1-derived phenyl radical; Luc-Bz-H, luciferin-6'-benzyl ether; Luc-Bz-NO_2, luciferin-6'-*p*-nitrobenzyl ether; Luc-Bz-OH, luciferin-6'-*p*-hydroxybenzyl ether; Luc-NO_2, 6'-nitroluciferin; Luc-OH, D-luciferin or firefly luciferin; Luc-OH-Cl, 7'-chloro-D-luciferin; Luc-OH-NO_2, 7'-nitro-D-luciferin; MeCN, acetonitrile; MNP, 2-methyl-2-nitrosopropane; MRM, multiple reaction monitoring; MS, mass spectrometry; NMR, nuclear magnetic resonance; $ONOO^-$, peroxynitrite; PCL-1, peroxy-caged luciferin; PEG, polyethylene glycol; PMA, phorbol 12-myristate 13-acetate; 2-PrOH, 2-propanol; QM, *para*-quinone methide; RNS, reactive nitrogen species; ROS, reactive oxygen species; SIM, single ion monitoring; TFA, trifluoroacetic acid

1. Introduction

Understanding the (patho)physiological role of reactive oxygen species/reactive nitrogen species (ROS/RNS) requires the availability of probes for their detection and (semi)quantitative analyses in the *in vitro* and *in vivo* settings. Bioluminescent imaging (BLI) is commonly used for sensitive monitoring of various biomolecular processes in cells and living animals [1-7]. The popularity of bioluminescence assays in biomedical research has resulted in significant progress in the syntheses of new luminescent analogs of luciferin [8] and luminogenic probes based on the firefly luciferin (Luc-OH) skeleton [9]. Among the caged probes, oxidant-sensitive luciferin derivatives have been reported for the detection of ROS/RNS in the *in vitro* and *in vivo* systems [10-15]. One of the first luciferin-based bioluminogenic probes designed to image hydrogen peroxide (H_2O_2) in living systems was peroxy-caged luciferin (PCL-1) (Scheme 1) [10]. The hydroxyl group of Luc-OH is alkylated by the boronobenzyl moiety in PCL-1, which prevents recognition of the probe by luciferase. H_2O_2 reacts slowly with PCL-1 ($k = 1.2\ M^{-1}\ s^{-1}$) [11], releasing Luc-OH and *p*-quinone methide (QM) (Scheme 1) [12]. Release of Luc-OH from PCL-1 is followed by its oxidation to oxyluciferin and the appearance of the bioluminescence signal in luciferase-transfected cells.

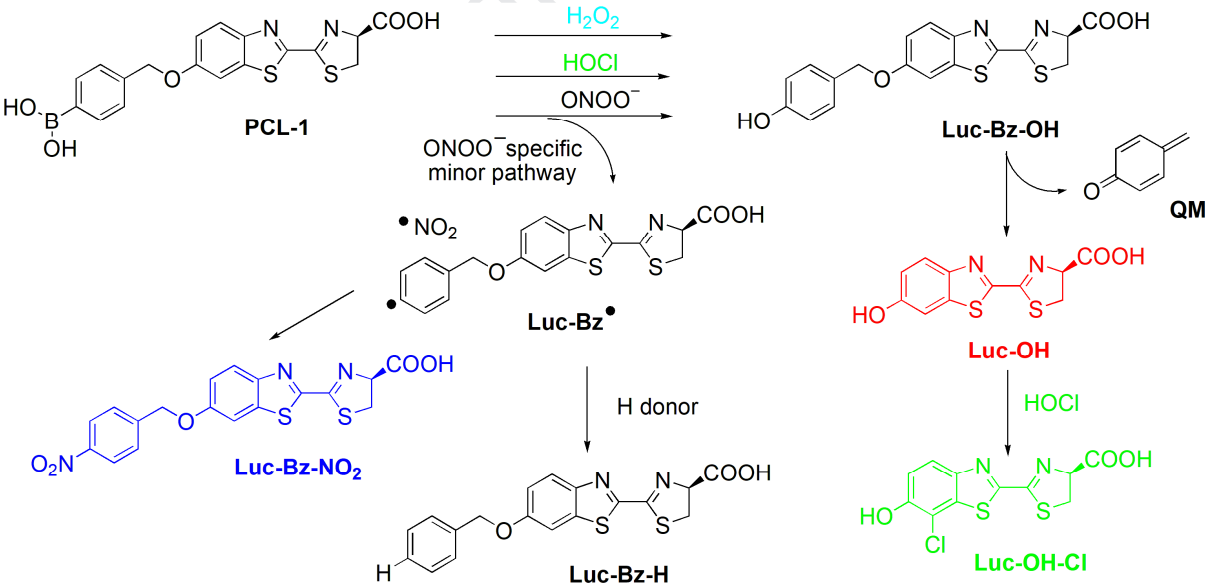

Scheme 1. Reaction of the PCL-1 probe with H_2O_2, HOCl, and $ONOO^-$, leading to the luminogenic substrate for luciferase (Luc-OH) after the release of QM, and to oxidant-specific products [10-12].

Recently, we have characterized in detail the reaction intermediates and stable products formed in the reaction between PCL-1 probe and selected inflammatory oxidants (H_2O_2, hypochlorous acid [HOCl], peroxynitrite [$ONOO^-$]) [12]. Similar to previously studied boronates [16,19,21,22], the reaction of PCL-1 with $ONOO^-$ proceeds *via* two pathways. The major pathway is the same as for H_2O_2 (Scheme 1) and involves the formation of the phenolic intermediate (Luc-Bz-OH), which after the elimination of QM yields Luc-OH as the stable end-product. The minor pathway produces nitrated and reduced products, Luc-Bz-NO_2 and Luc-Bz-H, respectively. [12]. We have demonstrated that $ONOO^-$-specific product, Luc-Bz-NO_2, is formed by activated macrophages incubated in the presence of the PCL-1 probe [12], which indicates that the PCL-1 probe can be applied to specifically detect and identify peroxynitrite in biological systems.

Hypochlorite is another oxidant that converts PCL-1 to Luc-OH [11,12]. Previously, it was shown that HOCl oxidizes boronate probes to nonspecific phenolic products [16, 17, 26]. However, the subsequent reaction of the phenolic product with HOCl yields chlorophenol(s), which can serve as a footprint for HOCl [16,17]. Reaction of PCL-1 with HOCl leads to the formation of Luc-OH, which may undergo subsequent chlorination to yield Luc-OH-Cl (Scheme 1) [12]. Therefore, Luc-OH-Cl detection, in addition to bioluminescence *in vivo*, may help identify HOCl as an oxidant responsible for the bioluminescence signal.

During the characterization of the PCL-1 probe, we identified some potential disadvantages of its use for the detection of oxidants in chemical, enzymatic, and/or biological systems, as follows: (*i*) During the uncaging of PCL-1 and other luciferin-based redox probes QM [10-12], quinoneimine [13], or benzoylhydrazine [15] are released. When probing the oxidant production on the scale of seconds or minutes, the self-immolation of those moieties may control the dynamics of the formation of the bioluminescent signal. (*ii*) QM, being an electrophile, may potentially affect the cellular redox status and, thus, affect the redox environment being probed. (*iii*) The PCL-1 probe decomposes significantly during prolonged incubation in a phosphate buffer (pH 7.4). Up to 50% of PCL-1 was lost (with Luc-OH detected as one of the products formed) over the 24-h incubation in the buffer [12]. This may translate into a high background bioluminescence signal, limiting the probe's sensitivity.

Here, we report the synthesis and characterization of a novel boronate-based luciferin derivative, LBE, with the boronate moiety attached directly at the site of the hydroxyl group (Scheme 2). Unexpectedly, this probe shows significantly higher stability, as compared with the PCL-1 probe, under the experimental conditions used to detect cell-based oxidants. In aqueous solutions containing a phosphate buffer (pH 7.4), we observed fast hydrolysis of LBE

to luciferin boronic acid (LBA). Compared with the PCL-1 probe, oxidation of LBA leads to instantaneous formation of luciferin, without any delay due to the requirement to eliminate the self-immolative QM moiety in PCL-1. This provides an opportunity for real-time monitoring of the dynamics of oxidant formation using the LBA probe, when coupled to fluorescence or bioluminescence detection, which produces lower background signal, as compared with the PCL-1 probe.

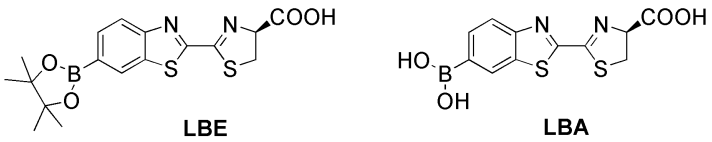

Scheme 2. Boronate-based luciferin derivatives

2. Experimental

2.1. General

2-Cyano-6-hydroxybenzothiazole (**1**), 2-cyanobenzothiazole (**6**), 2-amino-6-nitro-benzothiazole (**12**), *N*-phenyl-bis(trifluoromethanesulfonimide), trietylamine, *D*-cysteine, bis(pinacolato)diboron, [1,1'-bis(diphenylphosphino)ferrocene]dichloropalladium(II), (Pd(dppf)Cl_2), 1,1'-ferrocenediyl-bis(diphenylphosphine) (dppf), zirconium(IV) oxynitrate hydrate, copper(II) chloride, polyethylene glycol (PEG), and isoamyl nitrite (isoAmONO) were purchased from Sigma-Aldrich (Poznan, Poland). Solvents used for syntheses were reagent grade. The structures of the LBE probe and all synthesized standards – Luc-H, Luc-OH, Luc-NO_2, Luc-OH-Cl, Luc-OH-NO_2 – were confirmed by nuclear magnetic resonance (NMR) spectroscopy and mass spectrometry (MS) (see *Supporting Information*). ^{1}H NMR and ^{13}C NMR spectra were recorded with a Bruker Avance DPX 250 and Bruker Avance 400 spectrometers at 250 or 400 MHz (^{1}H) and 100 MHz (^{13}C), respectively. Compounds were dissolved in $CDCl_3$ or DMSO-d_6 and tetramethylsilane was added as internal reference for ^{1}H NMR and ^{13}C NMR spectra, respectively. Chemical shifts (δ) are reported in ppm, and coupling constant J values in hertz (Hz). The electrospray ionization (ESI)-MS spectra were recorded on a Finnigan MAT 95 spectrometer (Thermo Fischer Scientific, USA).

The stock solutions of oxidants (HOCl, and H_2O_2) were prepared freshly before each experiment and theirs concentrations were determined by spectrophotometry, using the procedure described previously [12]. Peroxynitrite was synthesized in reaction of 0.6 M nitrite with 0.7 M hydrogen peroxide at pH 13 [12]. Excess H_2O_2 was removed by passage through a column of MnO_2 and the solution was frozen at -20 °C. The liquid over the frozen solid was collected, aliquoted into 1.5 mL tubes and stored at −80 °C. The concentration of

peroxynitrite was determined spectrally at 302 nm ($\varepsilon 302 = 1.7\times10^3\ M^{-1}cm^{-1}$), after dilution in 0.1 M NaOH to ~10 mM concentration, immediately prior to each experiment.. When studying LBE oxidation by HOCl, the LBE stock solution (1 mM) in acetonitrile (MeCN) was added to phosphate buffer (100 mM, pH 7.4) to receive a final concentration of 100 µM of the probe. Dimethyl sulfoxide (DMSO) solvent was avoided due to known rapid quenching of HOCl by DMSO [12, 33]. For other experiments, stock solutions of LBE were prepared in DMSO at 10 mM concentration, and this solution was added directly to the buffer to obtain the desired concentration. High performance liquid chromatography (HPLC) analyses indicate that LBE (pinacolate ester) undergoes fast hydrolysis to the boronic acid form (LBA) upon dilution in the aqueous phosphate buffer. Therefore, although we added LBE to the reaction mixtures, LBA is the species that reacted with the oxidants tested.

2.2. Synthesis

All synthetic pathways are shown in condensed form in Scheme 2. Detailed synthetic procedures and ^{1}H and ^{13}C NMR spectra are included in Supporting Information.

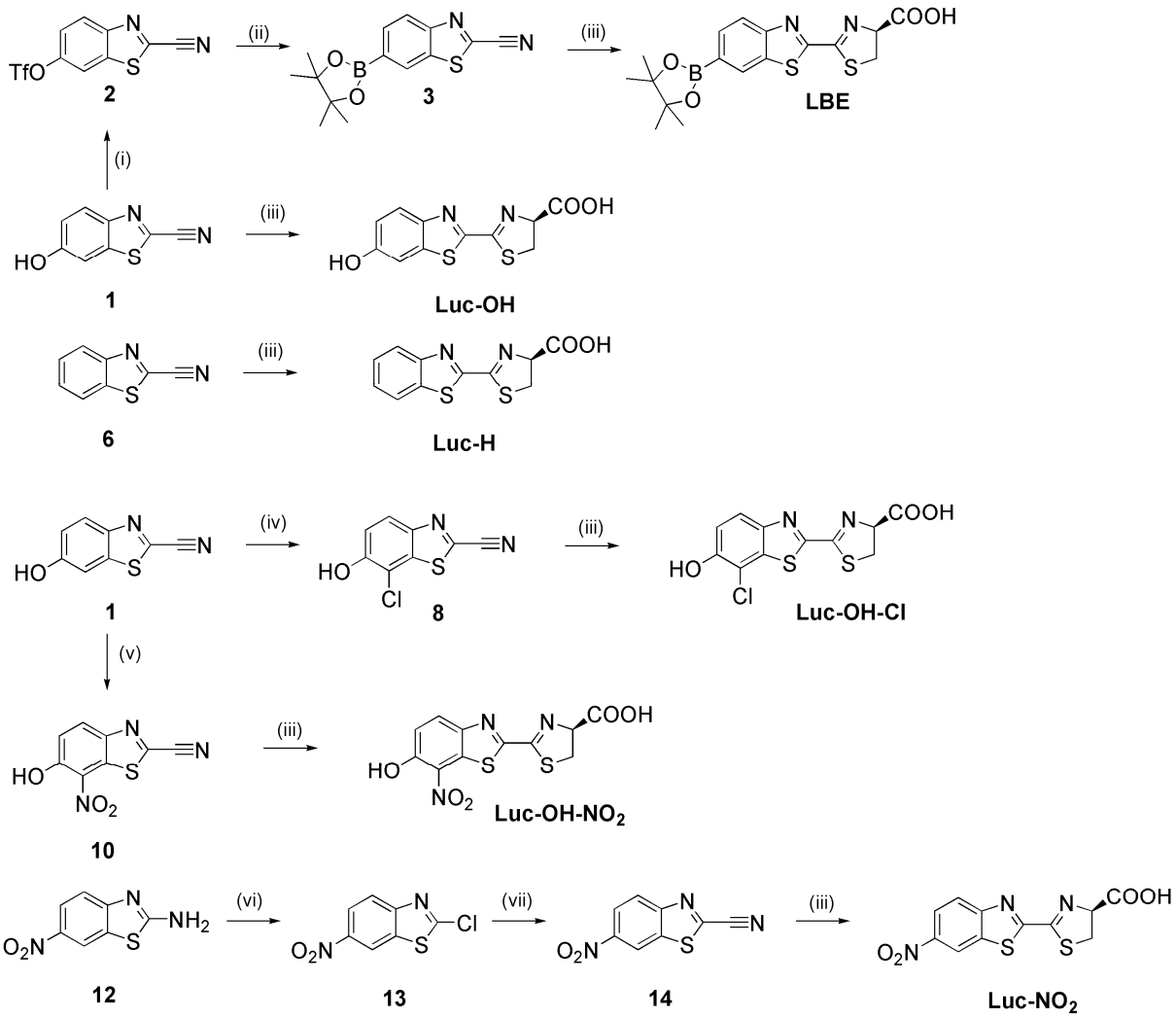

Scheme 3. Synthetic pathways used to obtain LBE probe and Luc-OH, Luc-H, Luc-OH-Cl, Luc-OH-NO_2, Luc-NO_2 standards. Reagents and conditions: (i): $PhN(SO_2CF_3)_2$, Et_3N, $CHCl_3$, Δ, 3 h; (ii): B_2pin_2, $Pd(dppf)Cl_2$, dppf, KOAc, 1,4-dioxane, 100 °C, microwave irradiation, Ar; (iii): *D*-Cys, K_2CO_3, MeOH/H_2O, 30 min; (iv): SO_2Cl_2, DCM, 16 h; (v): $ZrO(NO_3)_2xH_2O$, acetone, 100 °C, microwave irradiation, Ar, 15 min; (vi): $CuCl_2$, PEG, isoAmONO, MeCN, 65 °C, Ar, 3 h; (vii): NaCN, DMSO, 110 °C, Ar, 5 h.

2.3. HPLC analyses

HPLC analyses of all synthesized derivatives of luciferin, namely LBE, LBA, Luc-H, Luc-OH, Luc-NO_2, Luc-OH-Cl, and Luc-OH-NO_2 were performed using UFLC Shimadzu equipped with UV–Vis absorption and fluorescence detectors. Analyses were done using a Kinetex C_{18} column (Phenomenex, 100 mm × 4.6 mm, 2.6 μm), which was equilibrated with 10% of MeCN in water, containing 0.1% trifluoroacetic acid (TFA). The analytes were eluted by an increase of MeCN concentration from 10–70% over 12 min at the flow rate of 1.5

mL/min. The LBA probe and all products formed in its reaction with H_2O_2, HOCl, and $ONOO^-$ was detected by monitoring the absorbance at 330 nm. Additionally, Luc-OH was monitored using the fluorescence detector with the excitation set at 330 nm and emission set at 520 nm.

2.4. Fluorescence spectra analyses

Collection of fluorescence spectra and spectroscopic characterization were performed using a FLS-920 spectrofluorometer (Edinburgh Instruments, UK). The response of the LBA probe to oxidants was investigated by fluorescence titration experiments in aqueous solutions, containing a 100 mM phosphate buffer (pH 7.4), 10 μM dtpa, and 20% MeCN. The probe (100 μM) was incubated with H_2O_2, HOCl, or $ONOO^-$ for 24 h, 15 min, and 5 min, respectively.

2.5. EPR spin-trapping experiments

The spin-trapping experiments were conducted utilizing 2-methyl-2-nitrosopropane (MNP) as a spin trap using a Bruker EMX electron paramagnetic resonance (EPR) spectrometer, as described previously [12, 21]. Typically, the EPR spectra were recorded immediately after a bolus addition of peroxynitrite (200 μM) to mixtures consisting of LBE (200 μM) and MNP (40 mM) in a phosphate buffer (100 mM, pH 7.4) containing dtpa (100 μM) and MeCN (5%). The instrument parameters were as follows: scan range, 150 G; time constant, 1.28 ms; scan time, 84 s; modulation amplitude, 1 G; modulation frequency, 100 kHz; receiver gain, 1×10^5; and microwave power, 20 mW. The spectra shown are the averages of 10 scans.

2.7. LC-MS analyses

Liquid chromatography-mass spectrometry (LC-MS) analyses of LBA, its oxidation products, and spin adducts, were performed as described previously [12] using a Shimadzu LC-MS 8030 triple quadrupole mass detector coupled with a Shimadzu Nexera 2 UHPLC system equipped with a Cortecs C_{18} column (Waters, 50 mm × 2 mm, 1.6 μm). The column was equilibrated with 10% of MeCN in water containing 0.1% of formic acid. To separate the reaction mixture, a gradient elution with increasing concentration of MeCN in the mobile phase from 10–80% over 4 min was used. The flow rate was set at 0.5 mL/min, and the flow was diverted to waste during the first minute and after 4 min, counting from the time of injection. LBA and luciferin were detected in their deprotonated forms in the negative mode using single ion monitoring (SIM), set at m/z values of 307 and 279, respectively. MNP and

Luc-MNP spin adduct were detected in their protonated forms in positive mode using SIM, set at m/z values of 88 and 352, respectively.

2.8. Real-time monitoring of peroxynitrite formation from activated RAW 264.7 macrophages

RAW 264.7 cells were cultured in Dulbecco's Modified Eagle Medium (DMEM) (Gibco) supplemented with 10% fetal bovine serum (Omega Scientific), 2 mM L-glutamine, 100 units/mL penicillin, and 100 µg/mL streptomycin antibiotic at 37 °C in 5% carbon dioxide and 95% air atmosphere. The cells were seeded in 96-well plates at a concentration of 2×10^4 cells (in 150 µl) per well and incubated at 37° C and 5% carbon dioxide overnight.

For stimulations of the cells to produce nitric oxide, cells were incubated for 8 h with LPS (0.5 µg/mL) and INF-γ (50 units/mL). To stimulate NADPH oxidase-dependent superoxide production, the cells were washed twice with DMEM medium and treated with phorbol 12-myristate 13-acetate (PMA, 1 µM) (Sigma Aldrich) in Dulbecco's phosphate-buffered saline (DPBS) buffer supplemented with sodium pyruvate (0.3 mM) and glucose (5.5 mM) (DPBS-GP) (Gibco). At the time of addition of PMA, PCL-1 or LBE probe (20 µM) was also added. Where indicated, L-*N*-nitroarginine methyl ester hydrochloride (L-NAME, 1 mM) (Cayman Chemical) or catalase (CAT, 1 kU/mL) (Sigma Aldrich) was added at the time of addition of PMA and the probe. For cell-based experiments, stock solutions of LBE and PCL-1 probes were prepared in DMSO at 10 mM concentrations, and their final concentrations were 20 µM. Thus, the final concentration of DMSO was kept minimal, < 0.3% (v/v), upon dilution. For the control samples, cells were treated with the probes in the absence of stimulators and inhibitors.

Oxidation of probes was monitored in a 96-well fluorescence plate reader. The 96-well plate with cells was placed immediately after the addition of DPBS-GP containing the probe with or without PMA, L-NAME, and CAT in a plate reader prewarmed to 37 °C. Total fluorescence intensities were acquired using a FLUOstar Omega plate reader (BMG LABTECH) equipped with the appropriate excitation and emission filters (λ_{ex}=355 nm, λ_{em}=520 nm). The instrument was kept at 37 °C during the measurements, and fluorescence intensity was read from the bottom of each well.

3. Results

3.1 Synthesis and spectroscopic properties of luciferin's derivatives

To test if direct luciferin boronation may improve the performance the probe for oxidant detection, we synthesized luciferin boronic acid pinacol ester LBE and the anticipated minor products of its reactions with $ONOO^-$ and HOCl (see Scheme 4). First, we conducted spectroscopic characterization of these products; the results are shown in Table 1. Among all the compounds tested, only Luc-OH and Luc-OH-Cl exhibited significant fluorescence. It is worth noting that under physiological pH conditions, chlorinated luciferin exhibits a higher fluorescence quantum yield than luciferin (Table 1, Supplementary Fig. 1A). The deprotonation of luciferin results in increased fluorescence yield [29], which we attribute to the increased acidity of luciferin upon chlorination. In fact, the reported pK_a values for Luc-OH and Luc-OH-Cl are 8.5 and 6.7, respectively [30].

Analyses of the fluorescence spectra recorded after reacting the LBE probe with H_2O_2, HOCl, and $ONOO^-$ (Supplementary Fig. 1B-D) indicate that fluorescent products are formed for all three oxidants. However, the concentration-dependence of the fluorescence intensity suggests some difference between the oxidants. While in the presence of excess H_2O_2, the fluorescence intensity does not change; in case of HOCl, the intensity further increases; and in the case of $ONOO^-$, the intensity decreases. Based on the determined spectroscopic properties of Luc-OH, Luc-OH-Cl, and Luc-OH-NO_2, these results suggest that luciferin formed upon oxidation of the LBA probe undergoes chlorination by excess HOCl [12,16,17] or nitration by excess $ONOO^-$ [16]. To better understand the chemical mechanisms of oxidation of the probe by those three oxidants, we performed detailed identifications and quantifications of the products formed.

Table 1. Spectroscopic properties of the **LBA** probe and the products of its reaction with the oxidants tested in aqueous phosphate buffer (100 mM, pH = 7.4):MeCN (4:1)

Compound	λ_{max} (nm)	ε (λ_{max}) ($M^{-1} \cdot cm^{-1}$)	λ_{exc} (nm)	λ_{em} (nm)	Φ_{em} (%)	Stokes shift (nm)
LBA	300	10 600	-	-	-	-
Luc-OH	328 (326 [a])	11 900 (10 700 [a])	334 (331 [a])	536 (417 [a])	43 (1 [a])	202 (86 [a])
Luc-H	298	14 500	-	-	-	-
Luc-NO_2	310	19 200	-	-	-	-
Luc-OH-Cl	390	14 300	391	532	67	141
Luc-OH-NO_2	434	7 200	-	-	-	-
	366	23 000				

[a] In pure MeCN

3.2. Identification of the primary product formed during the oxidation of LBA

The spectroscopic data presented in Table 1 indicate that although the nitration products are non-fluorescent, chlorination of luciferin yields a highly fluorescent product. Therefore, the quantitative detection of inflammatory oxidants especially of HOCl and $ONOO^-$, based solely on fluorescence intensity measurements, may be inadequate. Moreover, it has been reported the presence of the chlorine atom in Luc-OH-Cl does not prevent the interaction with luciferase, but that it affects the bioluminescence signal intensity [30]. Thus, similar to the PCL-1 probe [12], the application the LBE probe for quantification of H_2O_2, HOCl, or $ONOO^-$ production *in vitro* or *in vivo* requires knowledge of the probe's chemistry, and should involve the identification of the oxidant-specific product(s). First, we identified the products formed during oxidation of LBE by three different biologically relevant, inflammatory oxidants known to oxidize boronic compounds.

3.2.1. Oxidation of LBA by H_2O_2

As mentioned, H_2O_2 oxidizes LBA to luciferin. The HPLC chromatograms presented in Fig. 1A show that Luc-OH is the sole product formed in this reaction. The slow reaction kinetics required a 24-h incubation period to ensure completion of the reaction between the probe and H_2O_2, when present at submillimolar concentrations. Stoichiometric analysis of the reaction between LBA and H_2O_2 is shown in Fig. 1B. Over the 24-h incubation period, LBA is stable in aqueous solution containing phosphate buffer (0.1 M, pH 7.4) and MeCN (20%), as indicated by the fact that almost 99% of the initial amount of LBA is still detected. Similar results were obtained in the phosphate buffer solution (0.1 M, pH 7.4) containing DMSO (1%). Stoichiometric analysis also shows that LBA is completely consumed by H_2O_2, and the maximum yield of Luc-OH was achieved when the probe was reacted with a small excess of the oxidant (less than 1.5 equivalents of H_2O_2), consistent with the 1:1 stoichiometry previously reported for mono-boronated probes [16, 19]. The yield of luciferin was ca. 96% and did not change in the presence of oxidant excess. Since probe purity was 98% and we identified Luc-H as an impurity, one can conclude that the reaction of LBA with H_2O_2 led to the formation of luciferin as the sole product.

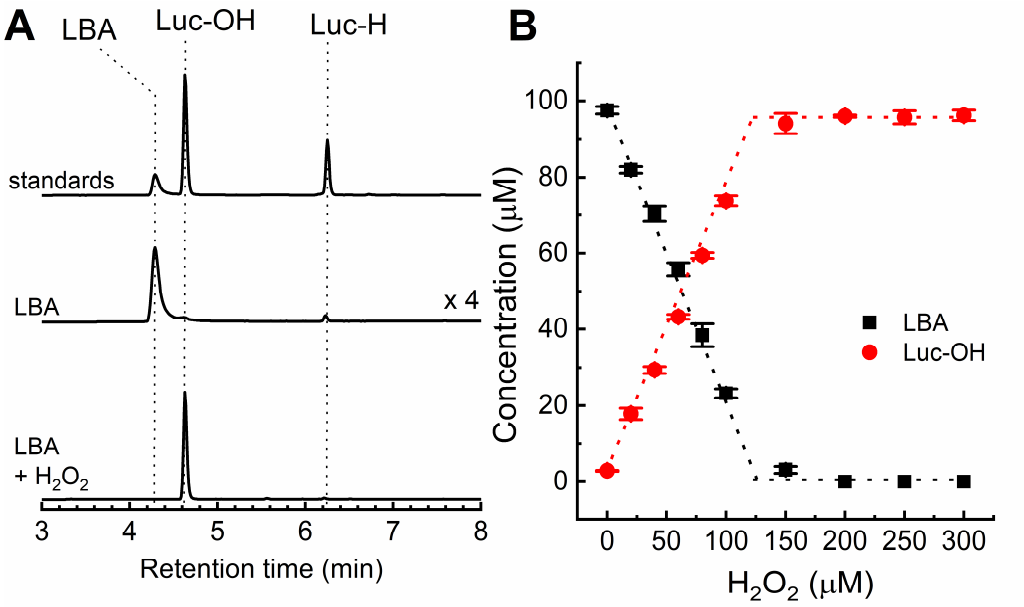

Figure 1. (A) HPLC chromatograms of the standards (100 µM each) and reaction mixtures of LBA (100 µM) with H_2O_2 (200 µM) after 24 h of incubation. The traces were collected using an absorption detector set at 330 nm. (B) HPLC-based titration of LBA (100 µM) with H_2O_2 after 24 h incubation in aqueous solution containing phosphate buffer (100 mM, pH 7.4), dtpa (10 µM), and MeCN (20%). Data are means ± standard deviation of three independent experiments.

3.2.2. Oxidation of LBA by HOCl.

HPLC chromatograms of the reaction mixtures of LBA with HOCl are presented in Fig. 2A. In addition to Luc-OH, a new product with a retention time of 5.7 min was formed during the reaction of the LBA probe with HOCl. The same product was formed when Luc-OH was mixed with HOCl. Comparison of the retention times of the synthesized authentic standard of 7'-chloroluciferin (Luc-OH-Cl) and the product formed in the reaction of LBA with HOCl confirms that Luc-OH-Cl is one of the products found in the reaction mixture. Formation of this product may explain why the maximum yield of Luc-OH reaches only ca. 60%. Luc-OH-Cl was previously found as a minor product of the reaction between of PCL-1 and HOCl [12]. The stoichiometric analysis of the oxidation reaction of LBA by HOCl is presented in Fig. 2B. The complete consumption of the probe and formation of luciferin requires use of more than 1.5 HOCl equivalents. Unlike the reaction of LBA with H_2O_2, an excess of HOCl causes disappearance of luciferin. This is consistent with our previous investigation using the PCL-1 probe, which demonstrated that released luciferin undergoes further reaction with HOCl, leading to the formation of Luc-OH-Cl, a product specific for HOCl.

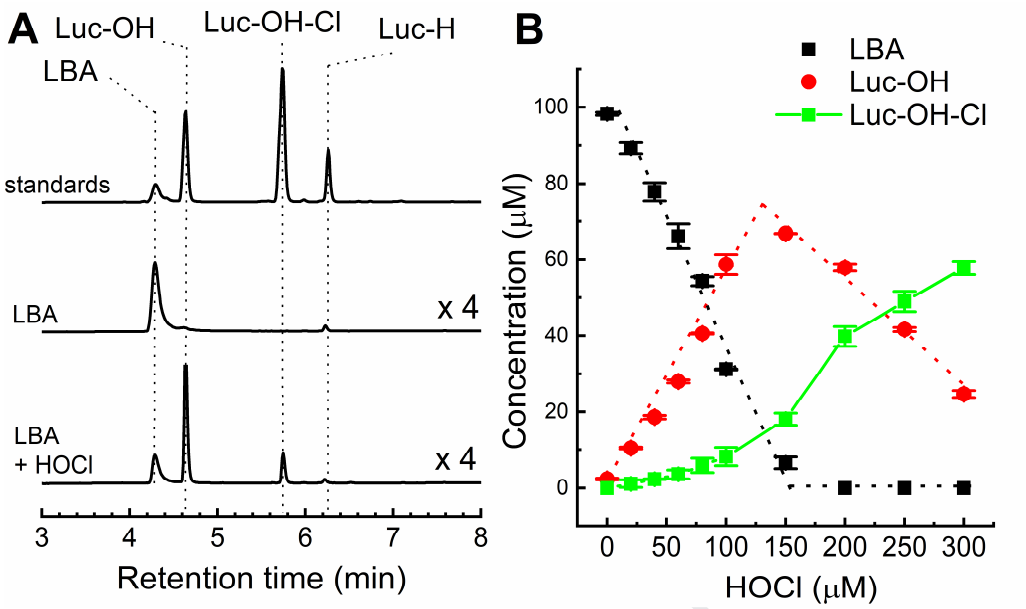

Figure 2. Reaction between LBA and HOCl in aqueous solution containing phosphate buffer (100 mM, pH 7.4), dtpa (10 μM), and MeCN (10%). (A) HPLC chromatograms of the standards (100 μM each) and reaction mixtures of LBA (100 μM) with HOCl (80 μM) after 15 min of incubation. The traces were collected using an absorption detector set at 330 nm. (B) HPLC-based titration of LBA (100 μM) with HOCl. Data are means ± standard deviation of three independent experiments

3.2.2. Oxidation of LBA by peroxynitrite

HPLC chromatograms and stoichiometric analyses of the reaction mixtures of LBA with $ONOO^-$ are shown in Fig. 3A and 3B, respectively. The results indicate that the main product of oxidation of the LBA probe by $ONOO^-$ is luciferin. Moreover, the yield of Luc-OH reached maximum (ca. 80% yield) when the LBA probe was reacted with an equimolar amount of $ONOO^-$, confirming a 1:1 reaction stoichiometry. Based on the two established pathways of oxidation of arylboronic acids by $ONOO^-$, we anticipated that the major (non-radical) pathway would yield luciferin and the minor (radical-mediated) pathway would yield Luc-NO_2 and Luc-H (see Scheme 2), the products derived from the phenyl-type radical formed [12, 21, 22]. Moreover, we expected that nitration of Luc-OH by $^{\bullet}NO_2$ formed in the minor pathway and during decomposition of excess $ONOO^-$ would produce Luc-OH-NO_2, as shown in Scheme 2. The chromatograms of the standards and of the reaction mixture confirmed the formation of Luc-H, Luc-NO_2, and Luc-OH-NO_2 when LBA was reacted with $ONOO^-$ (Fig. 3A).

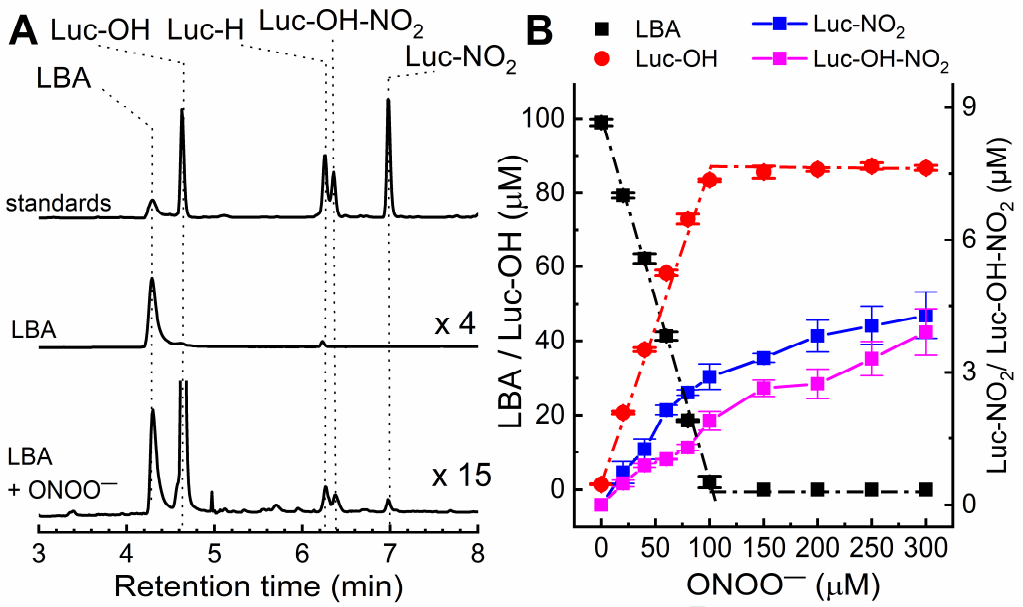

Figure 3. Reaction between LBA and $ONOO^-$ in aqueous solution containing phosphate buffer (100 mM, pH 7.4), dtpa (10 μM), and DMSO (1%). (A) HPLC chromatograms of the standards (100 μM each) and reaction mixtures of LBA (100 μM) with $ONOO^-$ (80 μM) after 5 min of incubation. The traces were collected using the absorption detector set at 330 nm. (B) HPLC-based titration of LBA (100 μM) with $ONOO^-$. Data are means ± standard deviation of three independent experiments.

The formation of minor products in the reaction mixture, anticipated for the radical pathway of the reaction, encouraged us to perform an EPR spin trapping experiment using an MNP spin trap. Reacting LBA with $ONOO^-$ in the presence of the MNP spin trap resulted in appearance of the EPR spectrum of the spin adduct, as shown in Fig. 4A (trace a). The intensity and resolution of this EPR signal are not sufficient to determine the g value and hyperfine coupling constants, but the signal clearly consists of three major lines (due to the hyperfine splitting from the nitrogen atom) with an additional structure (due to the hyperfine splitting caused by the phenyl ring hydrogen atoms). The addition of a bolus amount of $ONOO^-$ to incubations containing LBA, MNP, and 10% of 2-PrOH, a known scavenger of phenyl radicals, resulted in significantly reduced intensity of the EPR signal (Fig. 4A, trace b). The EPR spectrum recorded with MNP in the reaction mixture of LBA with $ONOO^-$ was not observed when any of those reaction components was absent (Fig. 4A, traces c and e). Unexpectedly, when $ONOO^-$ was added to a solution of LBE in the buffer and DMSO (in the

absence of the MNP spin trap), a single line was detected (Fig. 4A trace d). A similar EPR spectrum was observed for a long-lived DMSO radical cluster generated in neat DMSO with a small amount of base [31].

To further confirm the formation of Luc$^{\bullet}$ and to identify the molecular structure of spin-trapped radical, we combined the spin trapping experiment with LC-MS analysis of the spin adduct. The LC-MS analyses (Fig. 4B) enabled detection of the MNP spin trap in the positive mode using SIM, set at an m/z value of 88, and LBA (m/z = 308) consistent with hydrolysis of the boronate ester in the buffer used. Luc-OH (m/z = 280) was detected in all cases when the LBA probe was mixed with $ONOO^-$. In the presence of LBA, $ONOO^-$, and MNP, the spin adduct of MNP and Luc$^{\bullet}$ radical was detected (Fig. 4B, m/z = 352, peak detected at 2.33 min). This peak can be assigned to the spin adduct present in the form of nitroxide and/or protonated nitrone. The spin-trapping technique combined with the LC-MS-based analysis of the molecular weight of the radical adduct confirm the formation of the phenyl radical during the oxidation of LBA by $ONOO^-$.

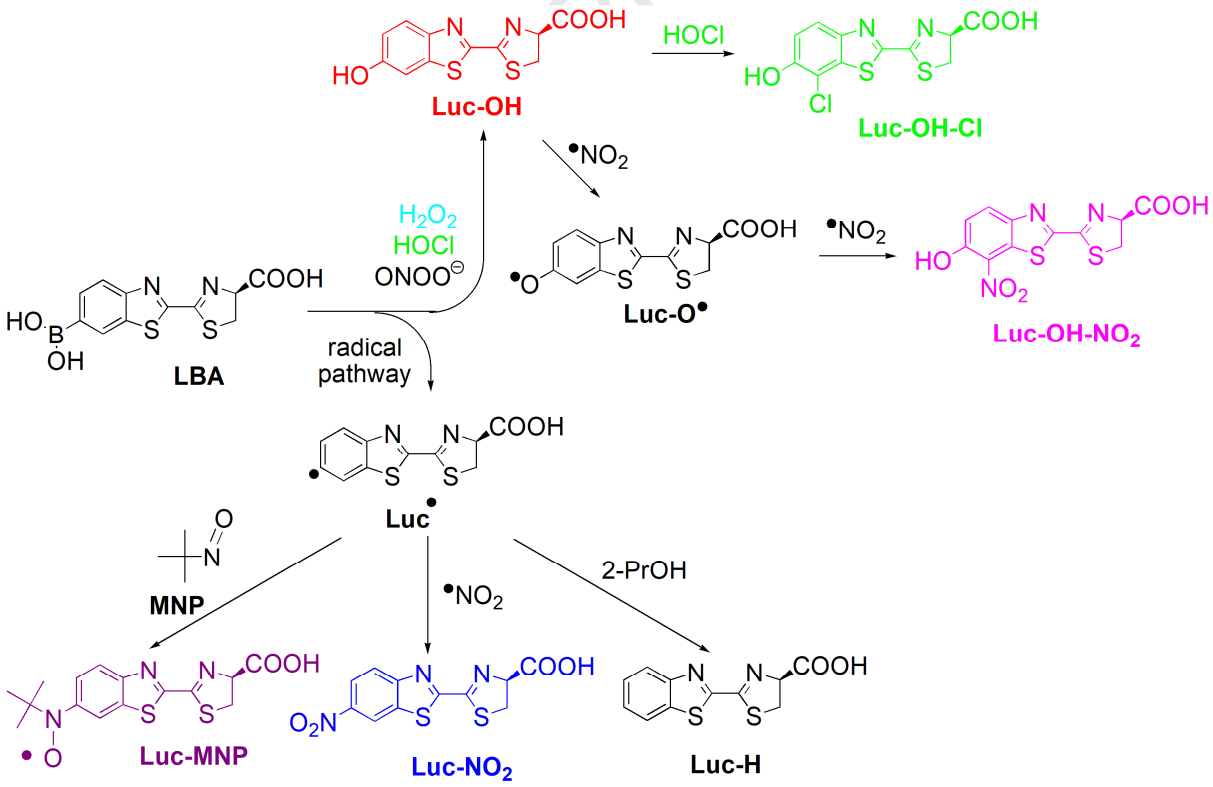

Scheme 4. Transformation of the LBA probe, leading to luciferin and $ONOO^-$-specific minor products. The colored structures of the stable products correspond to the color coding of the product profiles shown for different oxidants in Figures 1-3.

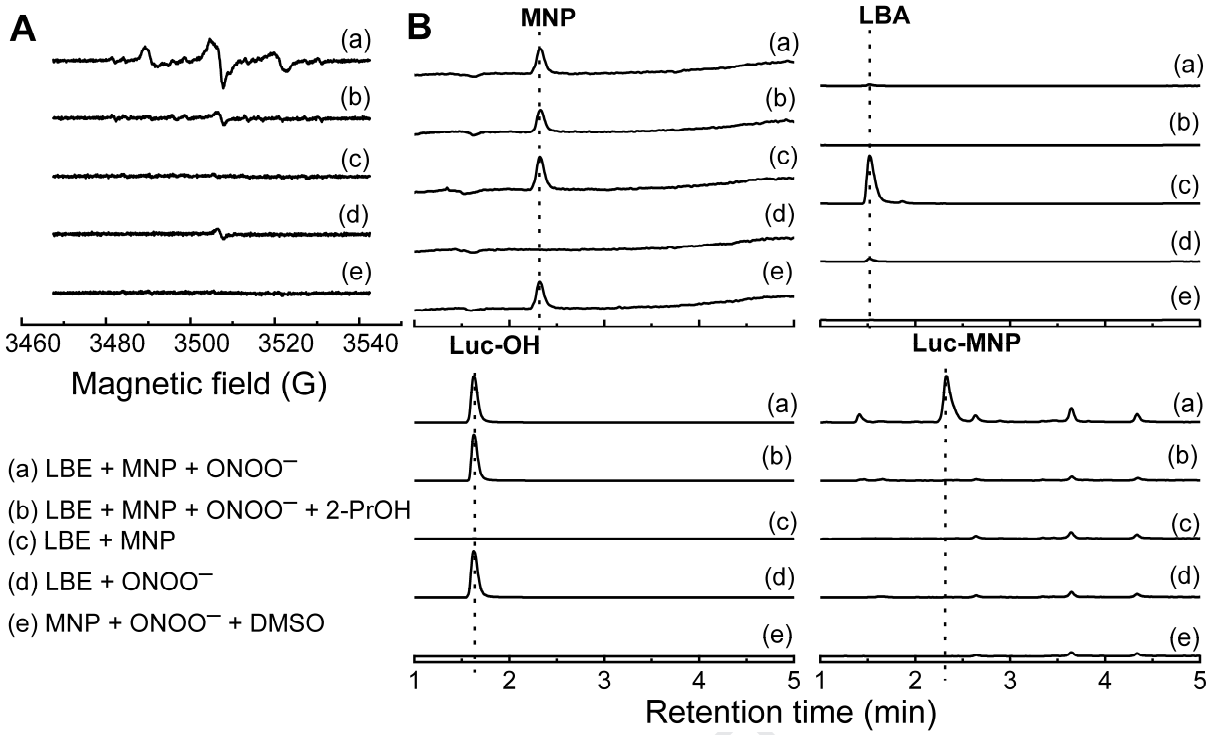

Figure 4. Spin trapping of the phenyl radical formed during the reaction of LBA with $ONOO^-$. (A) EPR spectra recorded using MNP as a spin trap. (B) LC-MS analyses of the luciferin boronic acid (LBA, $M\text{-}H^+$, m/z = (-)307), luciferin (Luc-OH, $M\text{-}H^+$, m/z = 279), MNP ($M+H^+$, m/z = (+)88), and Luc-MNP ($M+H^+$, m/z = (+)352) spin-adduct. $ONOO^-$ was added to the mixture of LBA (200 μM) and MNP (40 mM) in phosphate buffer (50 mM, pH 7.4) containing dtpa (10 μM), MeCN (5%), and DMSO (2.5%). The reaction mixture was transferred to an EPR capillary immediately after a bolus addition of $ONOO^-$, and the spectra were recorded at room temperature. Experiments were repeated three times independently. Representative result displayed.

We also analyzed the reaction mixture from the spin trapping experiments to detect $ONOO^-$-specific minor products. Figure 5 shows the product analyses of the oxidation of LBA by $ONOO^-$. The major product Luc-OH (Fig. 5, m/z = (-)279, peak detected at 1.61 min) is always detected when the LBA probe is mixed with $ONOO^-$. However, the yields of the nitrated products Luc-NO_2 (Fig. 5, m/z = (-)308, peak detected at 2.19 min), Luc-OH-NO_2 (Fig. 5, m/z = (-)325, peak detected at 2.02 min) and of the $Luc^{\bullet}$ reduction product, Luc-H, (Fig. 5, m/z = (-)263, peak detected at 2.04 min) depend on the composition of reaction mixture. When MNP is in the reaction mixture (Fig. 5, traces a), the yields of nitrated luciferins (Luc-NO_2, Luc-OH-NO_2) are significantly lower compared with the yields of the same products when oxidation was performed in the absence of MNP (Fig. 5, traces d). The addition of 2-propanol (2-PrOH) into the reaction mixture suppressed the formation of Luc-NO_2 and Luc-OH-NO_2 (Fig. 5, traces b) but increased the amount of Luc-H formed to the

level observed when LBA was oxidized by $ONOO^-$ in solution without a spin trap (Fig. 5, traces d). Together with the observed inhibitory effects of 2-PrOH on the formation of the phenyl radical spin adduct (Fig. 4), these data strongly point to the role of 2-PrOH as the quencher and reductant of the phenyl-type radical formed from the LBA probe. These observations are consistent with the occurrence of a minor radical pathway that is specific to the reaction between $ONOO^-$ and LBA. Overall, the EPR spin trapping experiments, the spin trapping combined with LC-MS analyses, and the effect of the phenyl radical scavengers on the product distribution demonstrate the involvement of the phenyl-type radical $Luc^{\bullet}$ in the minor pathway of the reaction of the LBA probe with $ONOO^-$.

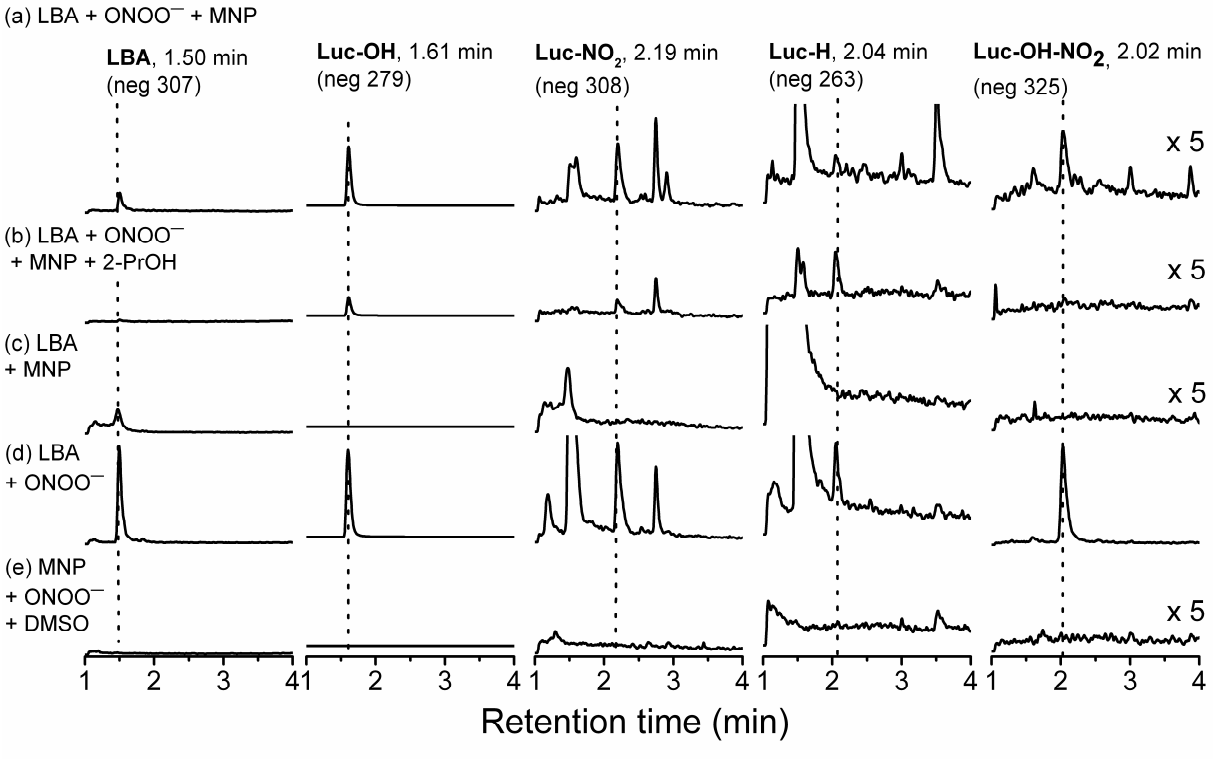

Figure 5. LC-MS analyses of the products of LBA oxidation by $ONOO^-$. The reactions were carried out under conditions similar to those described in Fig. 4. LC-MS traces of the reaction mixtures of (a) LBA (200 μM), MNP (40 mM), $ONOO^-$ (200 μM); (b) LBA (200 μM), MNP (40 mM), $ONOO^-$ (200 μM), 2-PrOH (10%); (c) LBA (200 μM), MNP (40 mM); (d) LBA (200 μM), $ONOO^-$ (200 μM); and (e) MNP (200 μM), $ONOO^-$ (200 μM), DMSO (2.5%). LBA, luciferin, Luc-NO_2, Luc-H, and Luc-OH-NO_2 were detected in negative mode using SIM set at m/z values of 307, 279, 308, 263, and 325, respectively. Experiments were repeated three times independently. Representative result displayed.

3.3. Limit of detection and quantification

Based on our HPLC analyses, we estimated the lowest concentrations of oxidant that are needed to detect the Luc-OH, Luc-OH-Cl, and Luc-OH-NO_2 (Supplementary Table 1). Results show that the detection limit of the LBA probe for $ONOO^-$, HOCl, and H_2O_2 was in the submicromolar to low micromolar range. Limits of detection of the $ONOO^-$-specific product Luc-NO_2 and hypochlorite-specific product Luc-OH-Cl were in the low micromolar range. As with other fluorescent products, the actual sensitivity will strongly depend on the detection modality and instrumentation. Furthermore, significantly higher sensitivity is expected in the case of bioluminescence-based detection of Luc-OH and Luc-OH-Cl, as observed for other luminescent probes.

3.4. Dynamics of the product formation

Formation of Luc-OH upon oxidation of the PCL-1 probe requires the release of the QM moiety from the primary oxidation product (Scheme 1). Therefore, to determine if this reaction may affect the dynamics of Luc-OH production, we compared the kinetic profiles of Luc-OH formation during the oxidation of LBA and PCL-1 to the profile of the product formation from a simple boronate probe, coumarin-7-boronic acid (CBA). Figure 6 shows the buildup of absorption at 380 nm during the reaction between those boronic probes and H_2O_2 (25 mM). It is evident that direct derivatization of luciferin using the boronate group results in a faster formation of the product (Luc-OH or 7-hydroxycoumarin) than when using the boronobenzylation approach, as in the case of the PCL-1 probe. The sigmoidal shape of the kinetic profile of the Luc-OH buildup observed in the case of the PCL-1 probe is consistent with a multistep process, following the kinetics of the formation of a product of two consecutive reactions.

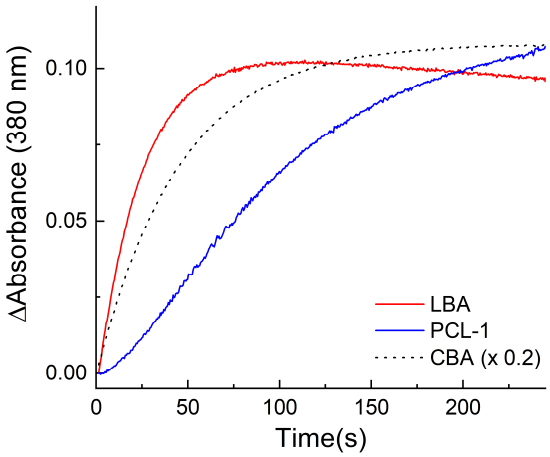

Figure 6. Kinetic profiles of product formation during the oxidation of probes LBA, PCL-1, and CBA (10 µM each) by H_2O_2 (25 mM). Experiments were repeated three times independently. Representative result displayed.

3.5. Oxidation of LBA and PCL-1 by activated macrophages

To confirm that the LBE probe can report $ONOO^-$ in biologically relevant cellular systems, we determined its performance in cultured RAW 264.7 cells activated to produce $ONOO^-$. RAW 264.7 macrophages were stimulated with a mixture of lipopolysaccharide (LPS), interferon γ (IFN-γ), and phorbol myristate acetate (PMA), as described previously [18,24]. In this cellular system, PMA activates NADPH oxidase to produce superoxide ($O_2^{\bullet-}$) whereas LPS/IFN-γ pretreatment induces expression of nitric oxide synthase (iNOS), resulting in increased production of $^{\bullet}NO$. Co-generation of both $O_2^{\bullet-}$ and $^{\bullet}NO$ leads to the formation of $ONOO^-$ and induces an increase in fluorescence intensity due to oxidation of LBE or PCL-1 boronate probe (Fig. 7A,B). The addition of LPS and IFN-γ or PMA alone to incubations containing macrophages and PCL-1 or LBE caused only a minor increase in fluorescence intensity (Fig. 7) as compared with the fully activated (LPS, IFN-γ, and PMA) cells. Interestingly, although both probes respond similarly to the treatments used, in case of untreated cells, a slow increase in the signal is observed for the PCL-1 probe but not for the LBE probe (Fig. 7, control). This indicates that LBA is more stable than PCL-1 under the experimental condition used.

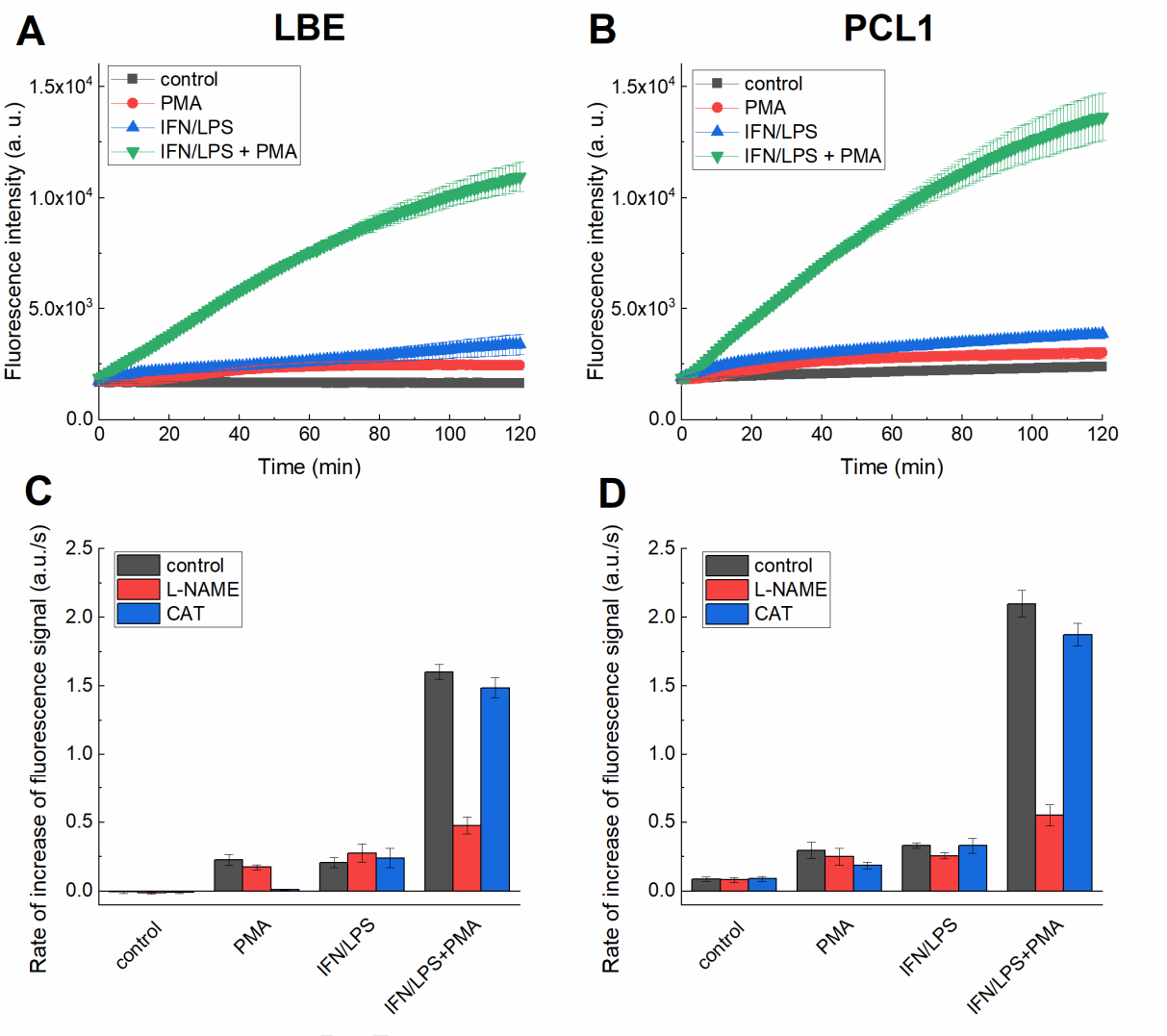

Figure 7. Real-time monitoring of the oxidation of the LBE (A) and PCL-1 (B) probes by activated RAW 264.7 macrophages. (C, D) Rate of increase in the fluorescence signal intensity from RAW 264.7 macrophages activated by different stimulators in the absence or in the presence of L-NAME and CAT. Incubations contained PCL-1 (20 µM) or LBE (20 µM) and RAW 264.7 macrophages in DBPS-GP buffer in different cellular conditions. Conditions were as follows: control cells, PMA added at the time of the measurement, LPS and INF-γ pre-treated cells, and LPS and INF-γ pre-treated cells with PMA added before measurements. (Details are described in the Experimental section.) Oxidation of the probes was followed by the measurement of the fluorescence intensity (λ_{ex} 355 nm, λ_{em} 520 nm).

To confirm the identity of the oxidants involved in the probes' oxidation, we tested the effect of L-NAME (iNOS inhibitor, preventing $ONOO^-$ formation) and catalase (H_2O_2 scavenger) on the rate of the probes' oxidation. As shown in Figs. 7C and 7D, L-NAME showed the strongest inhibitory effects when cells were coexposed to PMA and LPS-/IFN-γ. Under those

conditions, catalase had only a minor effect. These results indicate that both luciferin-based boronic probes tested can be used for real-time detection of $ONOO^-$ formed from macrophages activated to co-generate $^{\bullet}NO$ and $O_2^{\bullet-}$. Interestingly, catalase completely inhibited LBE probe oxidation in cells treated with PMA. This indicates that under these conditions H_2O_2 is the major oxidant.

4. Discussion

The application of probes to detect biologically relevant oxidants in inflammatory processes occurring *in vitro* and *in vivo* requires a detailed knowledge of probes' chemical reactivity, their stability in medium, and identification of the oxidant-specific product(s) together with their spectroscopic characterization. The PCL-1 probe represents the first boronate-based sensor to detect oxidants *in vivo* using the bioluminescence imaging modality [10]. Recently, we reported the application of the PCL-1 probe to monitor oxidants in tumor tissues *in vivo* in the mouse xenograft model of breast cancer, in combination with low-temperature EPR analyzes of inactivated aconitase signals [39]. Our recent investigation of the oxidation chemistry of the PCL-1 probe [12] showed that boronobenzylated luciferin (PCL-1 probe) decomposes significantly in phosphate buffer during prolonged incubation. This may lead to a relatively high background signal preventing the probe from detecting small, physiologically relevant levels of the oxidants. Here, we show that direct boronation of luciferin results in a more stable probe, LBE, which may represent a better choice when lower levels of the oxidants are to be detected.

Over the last decade, several reports and reviews have emphasized that it is impossible to categorically identify specific oxidants formed in cells without the application of HPLC- or LC-MS-based methods to detect oxidant-specific product(s) [12, 20, 32-37]. For example, 2-hydroxyethidium (a fingerprint of the reaction between hydroethidine and superoxide) and ethidium (nonspecific product of two-electron oxidation of hydroethidine by various oxidants) have overlapping fluorescence emission spectra but can be separated, identified, and quantified with the aid of HPLC or LC-MS, using appropriate standards [38]. The most promising probes for the detection of several nonradical ROS/RNS, produced under inflammatory conditions, are based on the oxidation chemistry of arylboronic acids or esters. Masking of hydroxyl or amino group(s) of a fluorophore by boronate or boronobenzyl moieties turns off the fluorescence [28]. Originally, this class of probes was developed for specific detection of H_2O_2 [28], which slowly uncaged the hydroxyl group and thus turned on the fluorescence [16,17]. Subsequent works proved that under physiological pH, boronate

probes are oxidized by HOCl and $ONOO^-$ at significantly higher rates than is the case for H_2O_2 [16]. The additional advantage of the fluorogenic boronate probes used to detect $ONOO^-$ is their ability to replace the boronate moiety by the $-NO_2$ (nitro) group and thus to form the $ONOO^-$-specific nitro derivatives [12,17,21]. In the presence of excess $ONOO^-$, the phenolic product may undergo nitration to form corresponding nitrophenol. Among the two nitration products, nitrobenzene-type (Luc-NO_2) and nitrophenol-type (Luc-OH-NO_2), only the nitrophenolic product can be formed via myeloperoxidase-catalyzed nitration. Since the nitrobenzene-type product is not generated during incubation of boronate probe with myeloperoxidase/H_2O_2/nitrite systems, its detection confirms the presence of $ONOO^-$ [16,24]. Bioluminescence imaging using luciferin-based probes is currently a standard technique for *in vivo* imaging. Based on our *in vitro* data with the use of activated macrophages, we predict that the LBE probe can be applied as a stable probe with low background for sensitive detection of ROS/RNS in *in vivo* animal models.

5. Conclusions

In this work, we synthesized the LBE probe, which undergoes hydrolysis to LBA in aqueous solutions. We have identified the products of LBA oxidation by selected inflammatory oxidants. The major, common product formed during the reaction of LBA with H_2O_2, HOCl, and $ONOO^-$ is luciferin, a substrate for bioluminescence imaging. However, oxidation of LBA by $ONOO^-$ proceeds *via* two pathways, with Luc-NO_2 being an $ONOO^-$-specific product formed in the minor pathway involving the phenyl-type radical $Luc^{\bullet}$ intermediate. Reaction of LBA with HOCl yields luciferin that is further chlorinated to Luc-OH-Cl, a product specific for HOCl. We propose combining LBA-based fluorescence or bioluminescence measurements with chromatographic analyses of those specific reaction products to identify the oxidants responsible for probe oxidation. Because the LBE probe is more stable than PCL-1, it may be a better choice for detecting inflammatory oxidants when present at low levels and/or when exhibiting slow reaction kinetics, such as H_2O_2.

Acknowledgment

This work was supported by a grant from the Polish National Science Centre within the SONATA BIS 6 program (Grant no. 2016/22/E/ST4/00549) to RP, a grant from the Polish National Science Centre within the MINIATURA 3 program (Grant no. 2019/03/X/ST4/00748) to MS, and an Institutional Research Grant IRG (#16-183-31) from the American Cancer Society and the Medical College of Wisconsin Cancer Center to JZ. The

LC-MS analyses were performed in Medical College of Wisconsin Cancer Center Redox and Bioenergetics Shared Resource.

References

[1] McCaffrey A, Kay MA, Contag CH. Advancing molecular therapies through in vivo bioluminescent imaging. Mol Imaging 2003;2:75-86. https://doi.org/10.1162/15353500200303124.

[2] Luker KE, Smith MCP, Luker GD, Gammon ST, Piwnica-Worms H, Piwnica-Worms D. Kinetics of regulated protein-protein interactions revealed with firefly luciferase complementation imaging in cells and living animals. Proc Natl Acad Sci USA 2004;101: 12288-12293. https://doi.org/10.1073/pnas.0404041101.

[3] d'Enfert C, Vecchiarelli A, Brown AJP. Bioluminescent fungi for real-time monitoring of fungal infections. Virulence 2010;1:174-176. https://doi.org/10.4161/viru.1.3.11119.

[4] Suff N, Waddington S. The power of bioluminescence imaging in understanding host-pathogen interactions. Methods 2017;127:69-78. https://doi.org/10.1016/j.ymeth.2017.07.001.

[5] Roy I, McAllister DM, Gorse E, Dixon K, Piper CT, Zimmerman NP, Getschman AE, Tsai S, Engle DD, Evans DB, Volkman BF, Kalyanaraman B, Dwinell MB. Pancreatic cancer cell migration and metastasis is regulated by chemokine-biased agonism and bioenergetic signaling. Cancer Res 2015;75:3529-3542. https://doi.org/10.1158/0008-5472.CAN-14-2645.

[6] Luwor RB, Stylli SS, Kaye AH. Using bioluminescence imaging in glioma research. J Clin Neurosci 2015;22:779-784. https://doi.org/10.1016/j.jocn.2014.11.001.

[7] Mezzanotte L, van't Root M, Karatas H, Goun EA, Löwik CWGM. Trends in Biotechnology 2017;35:640-652. https://doi.org/10.1016/j.tibtech.2017.03.012.

[8] Podsiadły R, Grzelakowska A, Modrzejewska J, Siarkiewicz P, Słowiński D, Szala M, Świerczyńska M. Recent progress in the synthesis of firefly luciferin derivatives. Dyes Pigm 2019;170:107627. https://doi.org/10.1016/j.dyepig.2019.107627.

[9] Li J, Chen L, Du L, Li M. Cage the firefly luciferin! - a strategy for developing bioluminescent probes. Chem Soc Rev 2013;42:662-676. https://doi.org/10.1039/c2cs35249d.

[10] Van de Bittner GC, Dubikovskaya EA, Bertozzi CR, Chang CJ. In vivo imaging of hydrogen peroxide production in a murine tumor model with a chemoselective bioluminescent reporter. Proc Natl Acad Sci USA 2010;107:21316-21321. https://doi.org/10.1073/pnas.1012864107.

[11] Sieracki NA, Gantner BN, Mao M, Horner JH, Ye RD, Malik AB, Newcomb ME, Bonini MG. Bioluminescent detection of peroxynitrite with a boronic acid-caged luciferin. Free Radic Biol Med 2013;61:40-50. https://doi.org/10.1016/j.freeradbiomed.2013.02.020.

[12] Zielonka J, Podsiadły R, Zielonka M, Hardy M, Kalyanaraman B. On the use of peroxy-caged luciferin (PCL-1) probe for bioluminescent detection of inflammatory oxidants in vitro and in vivo – Identification of reaction intermediates and oxidant-specific minor products. Free Radic Biol Med 2016;99:32-42. https://doi.org/10.1016/j.freeradbiomed.2016.07.023.

[13] Wu W, Li J, Chen L, Ma Z, Zhang W, Liu Z, Cheng Y, Du L, Li M. Bioluminescent probe for hydrogen peroxide imaging in vitro and in vivo. Anal Chem 2014;86:9800-9806. https://doi.org/10.1021/ac502396g.

[14] Kojima R, Takakura H, Kamiya M, Kobayashi E, Komatsu T, Ueno T, Terai T, Hanaoka K, Nagano T, Urano Y. Development of a sensitive bioluminogenic probe for imaging highly reactive oxygen species in living rats. Angew Chem Int Ed 2015;54:14768-14771. https://doi.org/10.1002/anie.201507530.

[15] Chen P, Zheng Z, Zhu Y, Dong Y, Wang F, Liang G. Bioluminescent turn-on probe for sensing hypochlorite in vitro and in tumors. Anal Chem 2017;89:5693-5696. https://doi.org/10.1021/acs.analchem.7b01103.

[16] Sikora A, Zielonka J, Lopez M, Joseph J, Kalyanaraman B. Direct oxidation of boronates by peroxynitrite: mechanism and implications in fluorescence imaging of peroxynitrite. Free Radic Biol Med 2009;47:1401-1407. https://doi.org/10.1016/j.freeradbiomed.2009.08.006.

[17] Zielonka J, Sikora A, Hardy M, Joseph J, Dranka BP, Kalyanaraman B. Boronate probes as diagnostic tools for real time monitoring of peroxynitrite and hydroperoxides. Chem Res Toxicol 2012;25:1793-1799. https://doi.org/10.1021/tx300164j.

[18] Zielonka J, Zielonka M, Sikora A, Adamus J, Joseph J, Hardy M, Ouari O, Dranka BP, Kalyanaraman B. Global profiling of reactive oxygen and nitrogen species in biological systems: high-throughput real-time analyses. J Biol Chem 2012;287:2984-2995. https://doi.org/10.1074/jbc.M111.309062.

[19] Zielonka J, Sikora A, Joseph J, Kalyanaraman B. Peroxynitrite is the major species formed from different flux ratios of co-generated nitric oxide and superoxide: direct reaction with boronate-based fluorescent probe. J Biol Chem 2010;285:14210-14216. https://doi.org/10.1074/jbc.M110.110080.

[20] Michalski R, Zielonka J, Gapys E, Marcinek A, Joseph J, Kalyanaraman B. Real-time measurements of aminoacid and protein hydroperoxides using coumarin boronic acid. J Biol Chem 2014;289:22536-22553. https://doi.org/10.1074/jbc.M114.553727.

[21] Sikora A, Zielonka J, Lopez M, Dybala-Defratyka A, Joseph J, Marcinek A, Kalyanaraman B. Reaction between peroxynitrite and boronates: EPR spin-trapping, HPLC analyses, and quantum mechanical study of the free radical pathway. Chem Res Toxicol 2011;24:687-697. https://doi.org/10.1021/tx100439a.

[22] Sikora A, Zielonka J, Adamus J, Debski D, Dybala-Defratyka A, Michałowski B, Joseph J, Hartley RC, Murphy MP, Kalyanaraman B. Reaction between peroxynitrite and triphenylphosphonium-substituted arylboronic acid isomers: identification of diagnostic marker products and biological implications. Chem Res Toxicol 2013;26:856-867. https://doi.org/10.1021/tx300499c.

[23] Zielonka J, Sikora A, Adamus J, Kalyanaraman B. Detection and differentiation between peroxynitrite and hydroperoxides using mitochondria-targeted arylboronic acid, In: Weissig V., Edeas M. (eds) Mitochondrial Medicine. Methods in Molecular Biology, vol 1264. Humana Press, New York, NY. http://doi.org/10.1007/978-1-4939-2257-4_16.

[24] Zielonka J, Zielonka M, VerPlank L, Cheng G, Hardy M, Ouari O, Ayhan MM, Podsiadly R, Sikora A, Lambeth JD, Kalyanaraman B. Mitigation of NADPH oxidase 2 activity as a strategy to inhibit peroxynitrite formation. J Biol Chem 2016;291:7029-7044. https://doi.org/10.1074/jbc.M115.702787.

[25] Smulik R, Debski D, Zielonka J, Michałowski B, Adamus J, Marcinek A, Kalyanaraman B, Sikora A. Nitroxyl (HNO) react with molecular oxygen and forms peroxynitrite at physiological pH: biological implication. J Biol Chem 2014;289:35570-35581. https://doi.org/10.1074/jbc.M114.597740.

[26] Shu W, Yan L, Wang Z, Liu J, Zhang S, Liu C, Zhu B. A novel visual and far-red fluorescent dual-channel probe for the rapid and sensitive detection of hypochlorite in aqueous solution and living cells. Sensor Actuat B-Chem 2015;221:1130-1136. https://doi.org/10.1016/j.snb.2015.07.066.

[27] Sedgwick AC, Han HH, Gardiner JE, Bull SD, He XP, James TD. Long-wavelength fluorescent boronate probes for the detection and intracellular imaging of peroxynitrite, Chem Commun 2017;53:12822-12825. https://doi.org/10.1039/c7cc07845e.

[28] Miller EW, Albers AE, Pralle A, Isacoff EY, Chang CJ. Boronate-based fluorescent probes for imaging cellular hydrogen peroxide. J Am Chem Soc 2005;127:16652-16659. https://doi.org/10.1021/ja054474f.

[29] Morton RA, Hopkins TA, Seliger HH. The spectroscopic properties of firefly luciferin and related compounds. An approach to product emission. Biochemistry 1969;8:1598-1607. https://doi.org/10.1021/bi00832a041.

654 [30] Takakura H, Kojima R, Ozawa T, Nagano T, Urano Y. Development of 5′- and 7′-
655 substituted luciferin analogues as acid-tolerant substrates of firefly luciferase, ChemBioChem
656 2012;13:1424-1427. https://doi.org/10.1002/cbic.201200142.
657 [31] Øpstad CL, Melø T-B, Sliwka H-R, Partali V. Formation of DMSO and DMF radicals
658 with minute amounts of base. Tetrahedron 2009;65:7616-7619.
659 https://doi.org/10.1016/j.tet.2009.06.109.
660 [32] Prolo C, Álvarez MN, Ríos N, Peluffo G, Radi R, Romero N. Nitric oxide diffusion to
661 red blood cells limits extracellular, but not intraphagosomal, peroxynitrite formation by
662 macrophages. Free Radic Biol Med 2015;87:346-355.
663 https://doi.org/10.1016/j.freeradbiomed.2015.06.027.
664 [33] Rios N, Piacenza L, Trujillo M, Martínez A, Demicheli V, Prolo C, Álvarez MN, López
665 GV, Radi R. Sensitive detection and estimation of cell-derived peroxynitrite fluxes using
666 fluorescein-boronate. Free Radic Biol Med 2016;101:284-295.
667 https://doi.org/10.1016/j.freeradbiomed.2016.08.033.
668 [34] Prolo C, Rios N, Piacenza L, Álvarez MN, Radi R. Fluorescence and chemiluminescence
669 approaches for peroxynitrite detection. Free Radic Biol Med 2018;128:59-68.
670 https://doi.org/10.1016/j.freeradbiomed.2018.02.017.
671 [35] Zielonka J, Kalyanaraman B. Small-molecule luminescent probes for the detection of
672 cellular oxidizing and nitrating species. Free Radic Biol Med 2018;128:3-22.
673 https://doi.org/10.1016/j.freeradbiomed.2018.03.032.
674 [36] Hardy M, Zielonka J, Karoui H, Sikora A, Michalski R, Podsiadły R, Lopez M, Vasquez-
675 Vivar J, Kalyanaraman B, Ouari O. Detection and characterization of reactive oxygen and
676 nitrogen species in biological systems by monitoring species-specific products. Antioxid
677 Redox Sign 2018;28:1416-14132. https://doi.org/10.1089/ars.2017.7398.
678 [37] Kalyanaraman B, Hardy M, Podsiadły R, Cheng G, Zielonka J. Recent developments in
679 detection of superoxide radical anion and hydrogen peroxide: Opportunities, challenges, and
680 implications in redox signaling. Arch Biochem Biophys 2017;617:38-47.
681 http://dx.doi.org/10.1016/j.abb.2016.08.021.
682 [38] Zielonka J, Hardy M, Kalyanaraman B. HPLC study of oxidation products of
683 hydroethidine in chemical and biological systems: ramifications in superoxide measurements.
684 Free Radic Biol Med 2009;46:329-338. https://doi.org/10.1016/j.freeradbiomed.2008.10.031.
685 [39] Cheng G, Pan J, Podsiadly R, Zielonka J, Garces AM, Machado LGDD, Bennett B,
686 McAllister D, Dwinell MB, You M, Kalyanaraman B. Increased formation of reactive oxygen
687 species during tumor growth: Ex vivo low-temperature EPR and in vivo bioluminescence

688 analyses. Free Radic Biol Med 2020;147:167-174.
689 https://doi.org/10.1016/j.freeradbiomed.2019.12.020.

Highlights

> Firefly luciferin-based probe for detection of peroxynitrite > Luciferin boronic acid (**LBA**) is oxidized to luciferin by H_2O_2, HOCl, and peroxynitrite > 7'-Chloroluciferin is a product specific for HOCl > 6'-Nitroluciferin serves as peroxynitrite-specific product > **LBA** enables real-time monitoring of the $ONOO^-$ formation in activated RAW 264.7 macrophages

Author Contributions

Radosław Podsiadły conceived and coordinated the study and wrote the paper; performed the EPR spin trapping experiments together with LC-MS detection of spin adducts

Marcin Szala synthesized **LBE** probe, its oxidation/nitration/chlorination/reduction products, designed, performed, analyzed, and interpreted the HPLC experiments, interpreted the NMR spectra,

Aleksandra Grzelakowska designed, performed, analyzed, and interpreted the data from real-time monitoring of peroxynitrite formation from activated RAW 264.7 macrophages

Julia Modrzejewska performed the spectroscopic and the HPLC experiments.

Przemysław Siarkiewicz performed the spectroscopic and the HPLC experiments

Daniel Słowiński performed the spectroscopic and the HPLC experiments

Małgorzata Świerczyńska performed the spectroscopic and the HPLC experiments

Jacek Zielonka designed, analyzed, and interpreted the EPR spin trapping experiments together with LC-MS detection of spin adducts, and revised the paper critically.

All authors reviewed the results and approved the final version of the manuscript.

Declaration of interests

☒ The authors declare that they have no known competing financial interests or personal relationships that could have appeared to influence the work reported in this paper.

☐The authors declare the following financial interests/personal relationships which may be considered as potential competing interests: